

Seismic performance assessment of a hybrid coupled wall system with replaceable steel coupling beams versus traditional RC coupling beams

Xiaodong Ji¹, Dan Liu¹, Ya Sun² and Carlos Molina Hutt³

¹*Department of Civil Engineering, Key Laboratory of Civil Engineering Safety and Durability of China Education Ministry, Tsinghua University, Beijing 100084, China*

²*China Architecture Design & Research Group, Beijing 100044, China*

³*Civil, Environmental and Geomatic Engineering, University College London (UCL), London WC1E6BT, UK*

SUMMARY

This study assesses the seismic performance of a hybrid coupled wall (HCW) system with replaceable steel coupling beams (RSCBs) at four intensities of ground motion shaking. The performance of the HCW system is benchmarked against the traditional reinforced concrete coupled wall (RCW). Nonlinear numerical models are developed in OpenSees for a representative wall elevation in a prototype 11-story building designed per modern Chinese codes. Performance is assessed via nonlinear dynamic analysis. The results indicate that both systems can adequately meet code defined objectives in terms of global and component behavior. Behavior of the two systems is consistent under service level earthquakes, whereas under more extreme events, the HCW system illustrates enhanced performance over the RCW system resulting in peak interstory drifts up to 31% lower in the HCW than the RCW. Larger drifts in the RCW are due to reduced coupling action induced by stiffness degradation of RC coupling beams, whereas the stable hysteretic responses and overstrength of RSCBs benefits post-yield behavior of the HCW. Under extreme events, the maximum beam rotations of the RSCBs are up to 42% smaller than those of the RC coupling beams. Moderate to severe damage is expected in the RC coupling beams, whereas the RSCBs sustain damage to the slab above the beam and possible web buckling of shear links. The assessment illustrates the benefits of the HCW with RSCBs over the RCW system, due to easy replacement of the shear links as opposed to costly and time consuming repairs of RC coupling beams.

KEYWORDS: hybrid coupled wall (HCW); replaceable steel coupling beam (RSCB); RC coupling beam; nonlinear dynamic analysis; seismic fragility; damage assessment.

1. INTRODUCTION

Recent earthquakes, including the 2008 Wenchuan earthquake (China), 2010 Maule earthquake (Chile), 2011 Tohoku earthquake (Japan) and 2011 Christchurch earthquake (New Zealand), have demonstrated that modern buildings generally behave well in terms of life safety. However, due to significant damage levels, post-earthquake repair of buildings is costly and time consuming, leading to a long-lasting loss of occupancy and a slow recovery of the community. In order to ensure minimal disruption in life and business in the urban society, prompt post-earthquake recovery of buildings is a clear need. One possible solution to achieve this goal is to use easily replaceable components, used as energy dissipation devices in which damage is concentrated (e.g., shear links, buckling restraint braces, etc.), while the remainder

of the structure is effectively undamaged.

Coupled wall systems are often used in high-rise buildings due to their superior strength and stiffness. In such a system, coupling beams distributed along the building height are designed as the components that undergo inelastic deformation and dissipate seismic energy. While traditional reinforced concrete (RC) coupling beams, if detailed appropriately show adequate seismic performance, once damaged, these components are expensive and time-consuming to repair. Recently, various types of replaceable coupling beams have been proposed and recognized as an alternative to traditional RC coupling beams (e.g., Fortney et al. [1], Christopoulos and Montgomery [2], and Ji et al. [3]).

A new type of replaceable steel coupling beam (RSCB), which comprises of a central “fuse” shear link connected to steel beam segments at its two ends is used in this study. By appropriately proportioning the beam segments and shear link, the inelastic deformation can concentrate in the “fuse” shear links during severe earthquakes, while the steel beam segments remain elastic. Extensive studies [4,5] have indicated that a short shear link with proper detailing can provide very stable, ductile and predictable behavior under cyclic shear loading. Recent tests by Ji et al. [3] have further demonstrated that the damaged link can be readily replaced by using specialized connections between the link and beam segments. Nevertheless, the seismic performance of a coupled wall system using the novel RSCBs has yet to be estimated.

The objective of this paper is to assess the seismic behavior, expected damage and reparability of a hybrid coupled wall (HCW) system consisting of RC wall piers and RSCBs. To illustrate the superior performance and benefit in reparability for the innovative HCW system, it is compared against a commonly-used reinforced concrete wall (RCW) with conventional RC coupling beams. To this end, Chapter 2 describes the design of coupled wall systems for assessment and the development of nonlinear numerical models for all structural components in the HCW and the RCW systems. Chapter 3 presents the intensities of ground shaking considered in the assessment and associated ground motion records selected for use in the nonlinear dynamic analysis. Chapter 3 also summarizes global and component responses of the HCW and the RCW systems subjected to various levels of earthquakes. Chapter 4 estimates the possible damage and reparability based on the seismic demands. The conclusions of this study are summarized in Chapter 5. Throughout this paper, the term HCW refers to a coupled wall consisting of RC wall piers and RSCBs, whereas the term RCW refers to a coupled wall with RC wall piers and RC coupling beams.

2. NONLINEAR NUMERICAL MODEL

2.1. Prototype structure and coupled wall system

2.1.1. Prototype structure. The prototype structure is an 11-story office building located in Beijing, adopting a RC frame-shear wall interacting system. The total height of the structure is 48.5 m, and the plan dimension is 48.6 m by 14.4 m. A representative floor plan is shown in Figure 1. The coupling beams in the transverse direction were designed as RSCBs, while the coupling beams in the longitudinal direction were designed as conventional RC coupling beams. The dead load of each story including the self-weight of the floor slabs and the

superimposed dead load varies from 5.5 kN/m^2 to 6.5 kN/m^2 . The live load is 2.5 kN/m^2 .

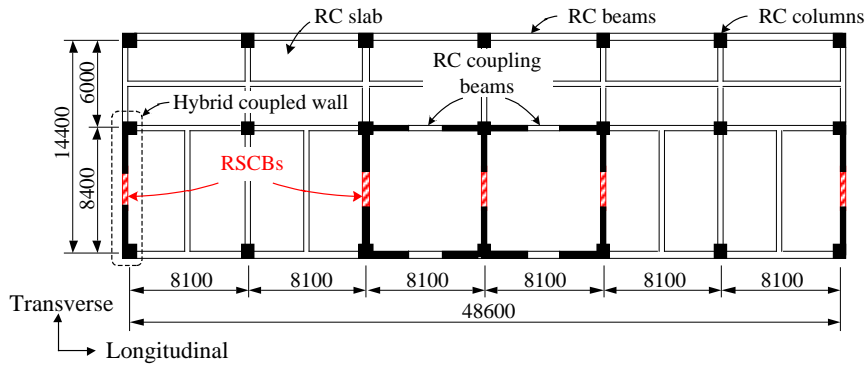


Figure 1. Plan view of prototype structure (units: mm).

The structure is designed according to the Chinese code for seismic design of buildings (GB 50011-2010) [6] and Chinese technical specification for concrete structures of tall buildings (JGJ 3-2010) [7]. Per the Chinese code requirements, the structure is designed to satisfy the strength demand of the service level earthquake (SLE, with a probability of exceedance of 63% in 50 years), which has a peak ground acceleration (PGA) of 0.07 g . Linear response spectrum analysis of a three-dimensional structural model is performed to determine the design forces of structural components and the deformation of the structure. In this analysis, a damping ratio of 5% is assumed for all modes. For the RC coupling beams, their effective flexural stiffness $E_c I_{\text{eff}}$ is taken as 15% of the stiffness value $E_c I_g$ based on gross section properties, to account for concrete cracking and slip and extension of the flexural reinforcement at the beam-wall interface, as recommended by Naish et al. [8]. The stiffness of the RSCBs is determined based on the gross section properties of shear links and beam segments. In accordance with GB 50011-2010, the elastic stiffness $E_c I_g$ is used for the RC wall piers and columns, as their deformations are small under SLE. The stiffness of RC frame beams is taken as $1.5 E_c I_g$ (for exterior beams) or $2.0 E_c I_g$ (for interior beams) as recommended by GB 50011-2010, to account for the increased stiffness contributed by above RC slabs. Under SLE, the Chinese code limits the interstory drift ratio to $1/800$ for RC frame-wall structures. This strict drift limit results in the design of relatively stiff buildings. The first three natural periods of the prototype structure are 1.57 s , 1.52 s and 1.32 s , corresponding to the vibration modes of translation in the transverse direction, translation in the longitudinal direction and the torsional mode, respectively. Under the SLE, the base shear coefficient of the structure is 5.3% and 5.5% in the transverse and longitudinal directions, respectively.

For a RC frame-wall interacting system, in general, seismic damage to RC frames is slighter than that of RC walls, because the walls often carry a dominated portion of the base shear force and overturning moment induced by seismic action and RC frames yield at a much larger drift than the RC walls. Nonlinear dynamic analysis of the prototype structure indicates that the RC frames sustain minor damage even under the maximum considered earthquakes (MCE), while seismic damage is concentrated within the coupled walls. This paper thus considers the coupled walls only for detailed analysis and performance assessment. The HCW on the left side of the prototype structure is selected for this study. Fig. 2 shows the geometry and detailing of the selected HCW. Gravity loads are applied to the HCW according

to its tributary area such that the gravity demands on the isolated HCW model and the three-dimensional structural model are consistent. The seismic masses in the isolated HCW are scaled such that the HCW has similar dynamic characteristics with the prototype structure in the transverse direction, as shown in Table I. Note that the two-dimensional analysis of the selected coupled wall does not include the additional seismic force induced by torsional effects in the prototype structure.

Table I. Dynamic properties of coupled wall and prototype structure in transverse direction.

Mode	Vibration period (s)			Mass participation factor		
	HCW	RCW	Prototype	HCW	RCW	Prototype
1	1.60	1.60	1.57	71.9%	71.9%	75.5%
2	0.38	0.38	0.42	16.1%	16.4%	13.5%
3	0.16	0.16	0.19	5.1%	4.7%	4.8%

An RCW with conventional RC coupling beams is also designed for comparison against the HCW with RSCBs. The RC coupling beams are designed to have nearly identical nominal shear strengths and effective stiffness as the RSCBs. The wall piers of the RCW are exactly the same as those of the HCW. The same gravity loads and masses are applied to the RCW.

2.1.2. Design of wall piers and coupling beams. When a coupled wall is subjected to lateral loads, the overturning moment is resisted by moment reactions developed at the base of the wall piers and coupling action induced by the coupling beams. Coupling ratio (CR) is defined as the proportion of overturning moment resisted by coupling action. In this paper, CR is calculated when all the coupling beams and wall piers yield. A rational amount of CR should be considered in the design of coupled walls. Harries [9] proposed a practical upper limit of 66% for the CR of coupled wall with steel coupling beams. El-Tawil and Kuenzli [10] recommends that the CR ranges from 30% to 45% for an efficient design. In this research, both the HCW and the RCW are designed to have a CR of 43%.

Figure 2 shows the dimensions and reinforcement layouts of the wall piers. The two boundary columns of prototype walls (as see in Figure 1) are ignored for simplicity of analysis, which does not affect the comparison of the two systems. C45 concrete (nominal axial compressive strength $f_{ck} = 29.6$ MPa) and HRB400 rebars (nominal yield strength $f_y = 400$ MPa) are adopted for the wall piers. The wall's boundary elements and reinforcement are designed to satisfy strength demand under SLE and the requirement of details specified by the GB 50011-2010 provisions. Note that, longitudinal reinforcement ratio in boundary elements is governed by the minimum code requirements, which results in flexural strength of the wall piers approximately twice the SLE demands.

The RSCBs shown in Figure 2 consist of a “fuse” shear link at the mid-span and two steel beam segments, which connect the ends of the shear link to the walls. Both the shear link and the beam segments adopt built-up I-shaped steel sections. Their cross-sectional dimensions are summarized in Table II. The strength of RSCBs is governed by the link strength, and it is designed to satisfy the strength demand under SLE. The link flanges are made of Q345 steel ($f_y = 345$ MPa), and the link webs of Q235 steel ($f_y = 235$ MPa). Use of hybrid sections with lower yielding strength steel in web is to promote early yielding in shear and to increase the

inelastic rotation capacity of links. The length of the shear link is assigned as 400 mm and the corresponding length ratio $e/(M_p/V_p)$ ranges from 0.59 to 0.77. Note that e denotes the length of shear link, and M_p and V_p denote the plastic flexural strength and shear strength of the link, respectively. Both the width-to-thickness ratios for link flange and web satisfy the requirement for highly ductile members by the AISC 341-10 [11] and GB 50011-2010 [6] provisions. According to AISC 341-10 [11], a shear link yields in shear if the length ratio is smaller than 1.6, and the plastic shear strength of the link is given by $V_n=0.6f_{y,w}A_w$, where $f_{y,w}$ denotes the yield strength of link web steel, A_w denotes the cross-sectional area of the link web. To ensure that the beam segments remain elastic when the shear link is fully yielded and strain-hardened, their strength is designed to exceed the strength demand corresponding to the overstrength of the shear link. The overstrength factor Ω of the shear link with a length ratio less than 1.0 is taken as 1.9 as suggested by Ji et al. [5]. Both the flanges and webs of steel beam segments are made of Q345 steel.

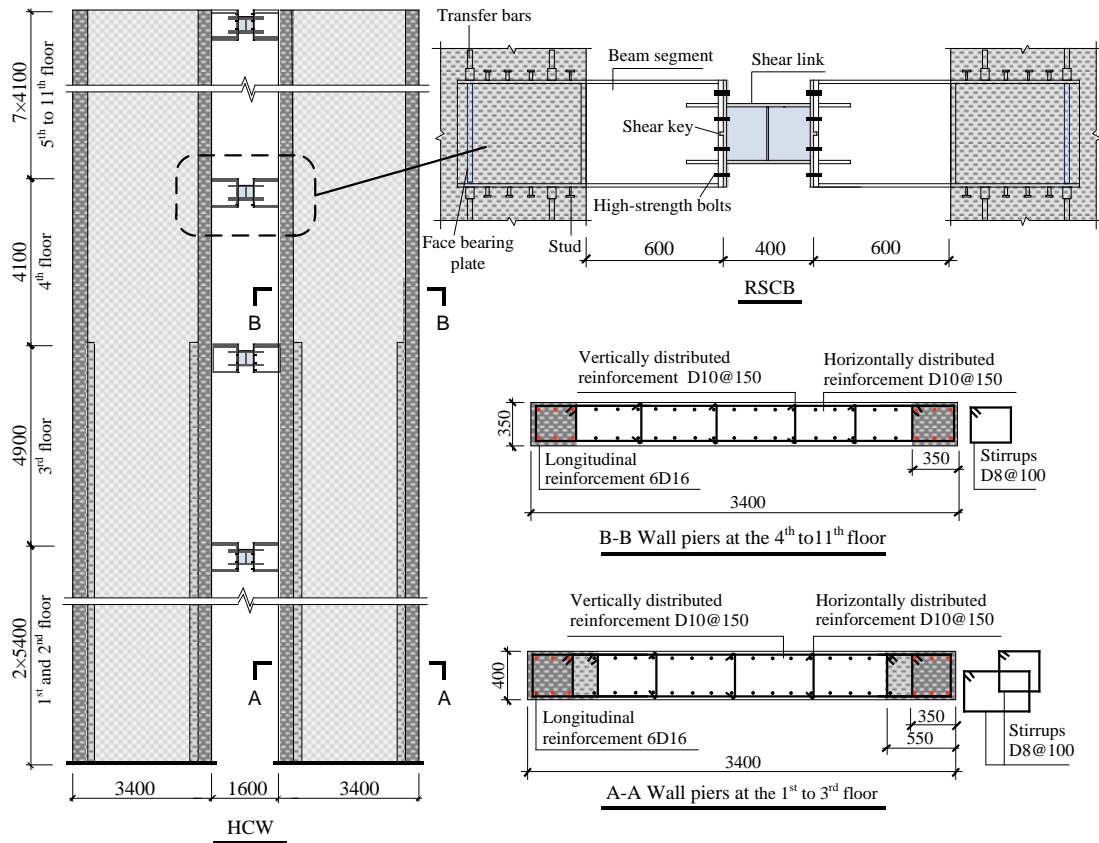


Figure 2. Wall dimensions and reinforcement details (dimensions are in mm).

Table II. Design parameters of RSCBs.

Component	Story	l (mm)	h (mm)	b_f (mm)	t_f (mm)	t_w (mm)	$\frac{h_w}{t_w}$	$\frac{b_f}{2t_f}$	$e/(M_p/V_p)$	V_p (kN)
Shear link	1	400	310	130	10	6	48.3	6.5	0.61	224
	2 to 3	400	370	130	10	8	43.8	6.5	0.73	361
	4 to 5	400	340	130	10	8	40.0	6.5	0.75	330

	6 to 7	400	320	130	10	8	37.5	6.5	0.76	310
	8 to 9	400	300	130	10	8	35.0	6.5	0.77	289
	10 to 11	400	350	130	10	6	55.0	6.5	0.59	255
Beam	1 to 3	600	550	150	14	8	79.1	7.3	-	-
segment	4 to 11	600	520	150	14	8	74.5	6.1	-	-

Notes: l denotes length of the component; h denotes height of the section; h_w denotes height of the web; b_f denotes width of the flange; t_w denotes thickness of the web; t_f denotes thickness of the flange; and V_p denotes the plastic shear strength of the component.

The shear link is connected to the beam segments using the end-plate connection with high-strength bolts and shear keys, as shown in Figure 2. The link-to-beam connection is designed such that the shear keys transfer the shear force and the high-strength bolts resist the bending moment. The strength of the connection is designed to exceed the overstrength capacity of the shear link. Ji et al. [3] demonstrated that this specialized link-to-beam connection can ensure favorable seismic behavior of the RSCBs and easy replacement of the shear links after being damaged in severe earthquakes. The embedded beam-wall connection design complies with the requirements for steel coupling beams in AISC 341-10 [11]. The connection strength is also designed to exceed the overstrength capacity of the shear link in order to ensure the joint would remain elastic even under severe earthquakes. The embedment length of coupling beams is determined using the design formulas specified in AISC 341-10 [11] to satisfy the strength of beam-wall connection.

In China, RC coupling beams are typically conventionally, rather than diagonally, reinforced. Therefore, conventional RC coupling beams are used in the RCW. The thicknesses of the RC coupling beams are the same as the thicknesses of the connected wall piers. The depth of the RC coupling beams is determined to provide the similar effective stiffness with the RSCBs. Table III summarizes the design parameters of the RC coupling beams. The Chinese code GB 50011-2010 recommends that RC coupling beams are designed to be governed by flexure to ensure adequate ductility, and therefore those beams in this study are designed to satisfy the “strong shear and weak bending mechanism”. The longitudinal reinforcement of the RC coupling beams is designed such that their nominal shear strength, $V_n = M_n/L$, is comparable to that of the RSCBs, where M_n denotes the yield flexural strength of RC coupling beams and L denotes the length of coupling beams.

Table III. Design parameters of RC coupling beams.

Story	b (mm)	h (mm)	L/h	Longitudinal reinforcement	Hoops (mm)	V_n (kN)	V_n/V_{cs}	$V_n / bh\sqrt{f'_c}$
1	400	600	2.67	3D16 + 1D18	D10@100	223	0.42	1.9
2 to 3	400	600	2.67	2D20+ 2D22	D10@100	361	0.68	3.0
4 to 5	350	600	2.67	5D18	D10@100	331	0.66	3.1
6 to 7	350	600	2.67	6D16	D10@100	314	0.62	3.0
8 to 9	350	600	2.67	3D16 + 2D18	D10@100	289	0.39	2.8
10 to 11	350	600	2.67	3D14 + 2D18	D10@100	252	0.29	2.4

Notes: b and h denote width and depth of the section, respectively; L denotes length of the coupling beam;

V_n and V_{cs} denote the nominal shear strength of the RC coupling beams and their shear strength capacity calculated per GB 50010-2010; f_c' denotes the axial compressive strength of the concrete in psi; the top and bottom longitudinal rebars in the coupling beams are symmetrical, and this table presents the rebars in either side.

2.2. RC wall pier modeling

The multi-layer shell element is adopted for modeling of the RC wall piers in OpenSees [12]. In the multi-layer shell element, the concrete cover and inside concrete are represented by a number of concrete layers, and the distributed reinforcements are represented by the smeared rebar layers in vertical and horizontal directions, respectively, as illustrated in Figure 3. The longitudinal rebars in the boundary elements are modeled with truss elements and they are coupled with the surrounding shell elements. Lu et al. [13] have implemented the multi-layer shell element in the computation platform OpenSees for modeling RC walls. Ji et al. [14] have validated the models by comparison with test results.

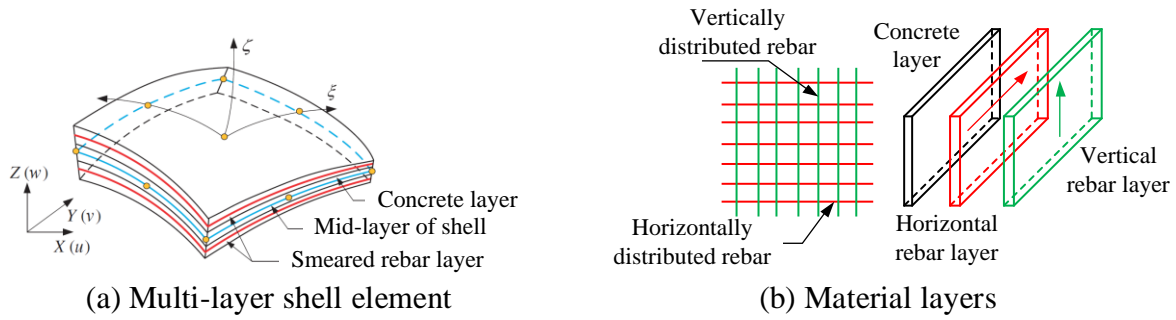


Figure 3. Sketch of multi-layer element for RC wall [13].

In the modeling, the concrete is assumed to behave in a plane-stress manner, and the cracking of the concrete is modeled by the fixed smeared crack approach. Well-calibrated models are used to represent the uniaxial compressive stress-strain relationship of the concrete. The concrete cover is represented by the Kent-Park model [15] and the stirrup-confined concrete by the Saatcioglu-Razvi model [16]. The uniaxial tensile stress-strain relationship of concrete is represented by a bilinear curve which takes into account the tension softening. The Giuffr -Menegotto-Pinto material model [17] is adopted to represent the uniaxial stress-strain relationship of the steel reinforcement. More details of parameter setting of the models can be found in [14].

2.3. Coupling beam modeling

2.3.1. Analytical RSCB model. Figure 4 shows the simplified numerical model for the RSCB. The shear link is simulated by a nonlinear link element. The mechanical behavior on each degree of freedom is modeled by a user-defined spring. In this case, the shear link is designed to yield in shear. Therefore the axial spring and flexural spring are elastic, while the shear spring is nonlinear. The properties of the axial, shear and flexural springs of the link element are listed in Table IV. Experiments [4,5] report that shear links present similar hysteretic performance with steel under cyclic loading. Therefore, the hysteretic behavior of the nonlinear shear spring is characterized by a uniaxial material model based on Giuffr -Menegotto-Pinto hysteretic model [17]. The parameters R_0 , cR_1 , cR_2 that reflect the

Bauschinger effect, the parameter b that reflects kinematic hardening effect and the parameters a_1 through a_4 that represent isotropic hardening effect are calibrated against experiment data. The values of these parameters are listed in Table IV as well. It should be mentioned that axial deformation and associated axial force develop in shear links when they experience large inelastic shear deformation [3,5], which may cause redistribution of shear forces of the wall piers that are connected to the RSCBs. However, the mechanism of the axial forces in shear links has yet to be clearly understood. In addition, the presence of RC slabs may suppress the influence of axial forces in shear links. Therefore, the study does not include the possible influence of axial forces in shear links.

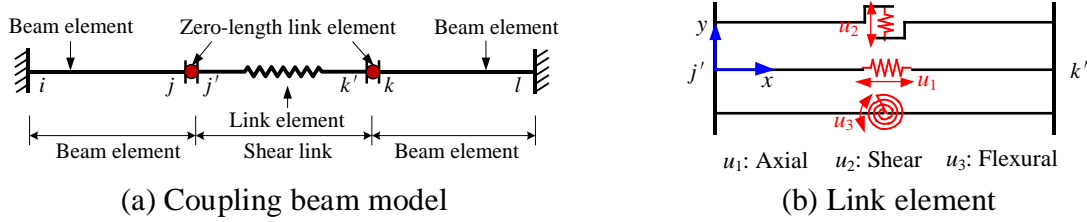


Figure 4. Nonlinear model for RSCB.

Table IV. Properties of the link element for shear links.

Springs	Parameters	Formulas or values
Elastic axial spring	Axial stiffness $K_{1,a}$	$K_{1,a} = EA_1 / e$
Elastic flexural spring	Flexural stiffness $K_{1,f}$	$K_{1,f} = EI_1 / e$
Nonlinear shear spring	Yield force $V_{1,y}$	$V_{1,y} = 0.6f_{y,w}A_{1,w}$
	Elastic stiffness $K_{1,s}$	$K_{1,s} = [e^3 / (12EI_1) + e / (GA_{1,w})]^{-1}$
	Parameters that control the transition from elastic to plastic branch	$R_0 = 18.5;$ $cR_1 = 0.9;$ $cR_2 = 0.1$
	Kinematic hardening ratio	$b = 0.003$
	Isotropic hardening parameter	$a_1 = a_3 = 0.14; a_2 = a_4 = 1.0$

Notes: E and G denote Young's modulus and shear modulus of the steel, respectively; e denotes length of the shear link; A_1 denotes the cross-sectional area of the shear link; I_1 denotes moment of inertia of the link section; $A_{1,w}$ denotes the cross-sectional area of the link web; $f_{y,w}$ denotes the yield strength of the link web.

The beam segment is designed to remain elastic under seismic action, and thereby it is modeled by an elastic beam element in OpenSees. This beam element does not include shear deformation, but shear deformation of short-span beam segments is not negligible. Therefore, a zero-length shear spring element is set between the beam element and the link element, for which the stiffness equals to the shear stiffness of beam segment, i.e., $k = GA_{b,w} / l_b$, where $A_{b,w}$ denotes the sectional area of the web of beam segment and l_b denotes the length of the beam segment.

2.3.2. *Verification of the RSCB model.* Both shear link experiments and RSCB experiments by Ji et al. [5,3] are modeled and analyzed cyclically to validate the numerical model developed for the RSCB. The analytical results compare well to the experimental results. Figure 5 shows the analytical and experimental force-displacement relationship of a shear link specimen and a RSCB specimen. More details of verification studies are reported in reference [18].

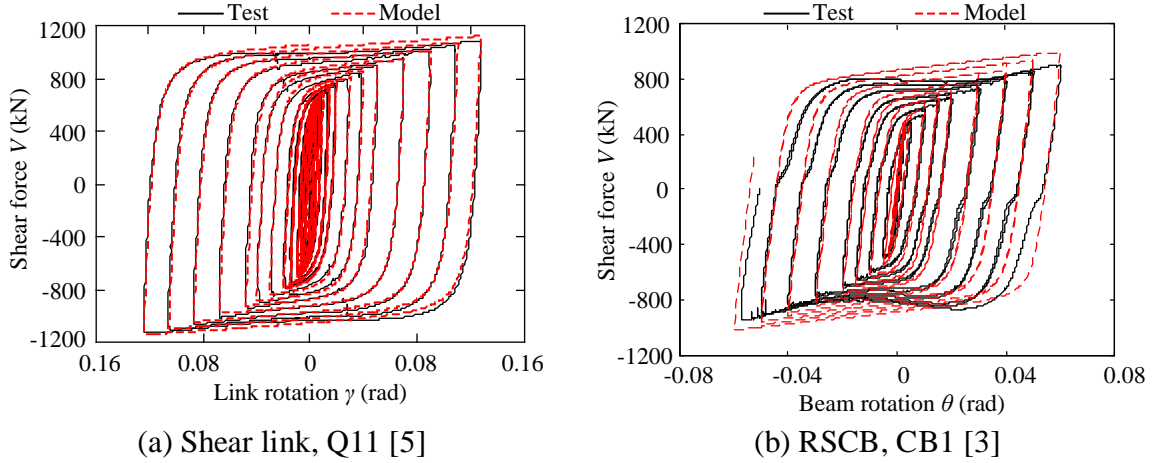


Figure 5. Comparison of experimental and analytical results of shear link and RSCB.

2.4. RC coupling beam model

RC coupling beams are modeled with a nonlinear link element. The skeleton of the force-displacement relationship of RC coupling beams is defined following the ASCE/SEI 41-13 provisions [19], as shown in Figure 6(a). θ denotes beam rotation, and V/V_n denotes normalized shear force of the coupling beam. The effective bending stiffness $E_c I_{\text{eff}}$ is taken as 15% of the stiffness value $E_c I_g$ based on gross section properties, as recommended by Naish et al. [8]. The ultimate strength (point C of the skeleton curve in Figure 6(a)) is taken as 1.15 times the yield flexural strength as reported in Kwan et al. [20]. Values of a , b and c depend on the failure mode and the nominal shear stress level $V_n / bh\sqrt{f'_c}$ of the RC coupling beams. Given the flexural failure mode and the values of $V_n / bh\sqrt{f'_c}$ listed in Table III, values a , b and c are calculated as 0.025 rad, 0.05 rad and 0.75 respectively according to the ASCE/SEI 41-13 provisions [19].

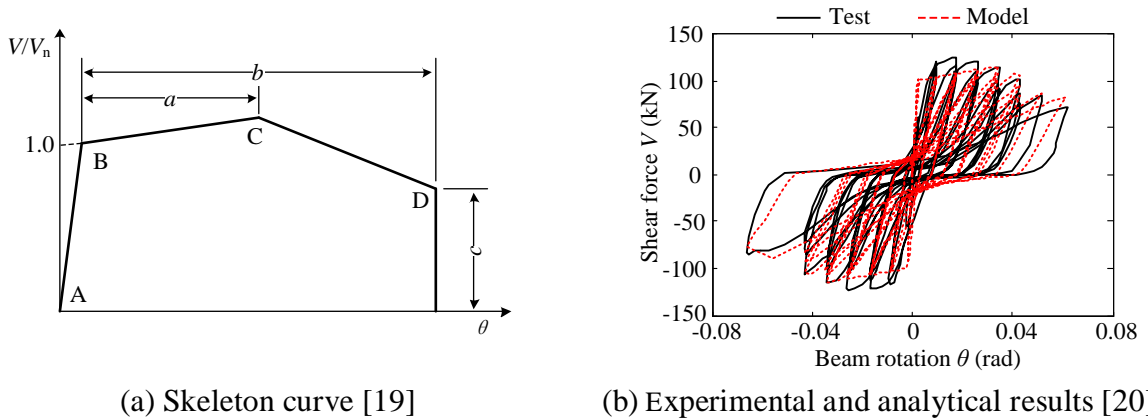


Figure 6. RC coupling beam modeling.

The hysteretic behavior, including the pinching effect, of conventional RC coupling

beams is related to the following three design parameters: the span-to-depth ratio, flexural-to-shear strength ratio V_n/V_{cs} and nominal shear stress level $V_n/bh\sqrt{f'_c}$ [21]. The test data of experimental specimens by Naish et al. [8] and Kwan et al. [20], which are similar to the RC coupling beams to be analyzed, are selected to calibrate the parameters of the hysteretic model that controls the unloading and reloading stiffness, pinching effect, etc. In general, the analytical results can track well the hysteretic curves obtained from the tests, of which one example is shown in Figure 6(b).

2.5. Beam-wall connection and slabs

The rigid connection between coupling beams and wall piers is modeled with additional rigid beam elements which transfer the forces developed at the coupling beam end to all wall shell elements at the coupling beam height. For the HCW, in fact, opening and closure of the gap between the embedded steel beams and RC wall piers may lead to additional nonlinearity. Pushover analysis with a sophisticated model that includes contact springs to reflect this nonlinearity at beam-wall connection indicates that the overall effect of gap opening and closure on the system behavior is small. Similar observation was found in Hassan and El-Tawil [22]. Considering the computational cost, the possible nonlinearity induced by gap opening and closure in beam-wall connection of the HCW is not considered in this study.

Ji et al. [23] recommended that the RC slabs are elevated from the RSCBs and reported that the elevated slab has limited influence on the initial stiffness, shear strength and hysteretic performance of the RSCB. Naish et al. [8] reported that the RC slabs could increase the nominal strength of RC coupling beams by 17%, while the slabs did not influence the ductility and hysteretic performance of RC coupling beams. As the coupled wall analyzed in this paper is an exterior wall, the effect of the RC slabs would be further decreased because the slabs are on one side of the RSCBs only. Therefore, the effect of RC slabs on coupling beams is ignored in the analysis.

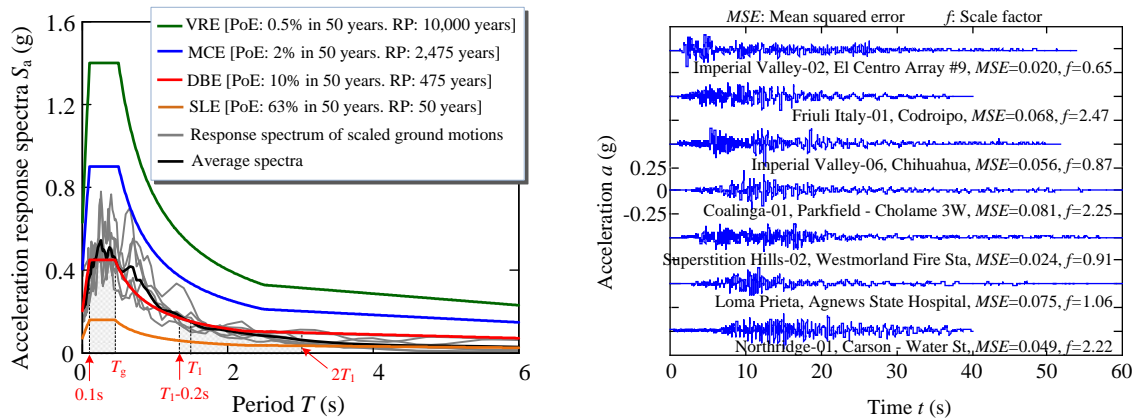
3. NONLINEAR RESPONSE TIME HISTORY ANALYSIS

3.1. Ground motions and dynamic analysis parameters

3.1.1. Intensities of ground motion shaking. Four intensities of ground motion shaking are considered for the performance assessment. These ground motion intensities are specified in the earthquake parameter zoning map of China (GB 18306-2015) [24]: service level earthquake (SLE), design basis earthquake (DBE), maximum considered earthquake (MCE) and very rare earthquake (VRE). The probabilities of exceedance and return periods for these intensities of shaking and the associated design response spectra are shown in Figure 7. The amplitudes of the SLE, MCE and VRE design spectra are 0.35, 2 and 3 times that of the DBE design spectrum, respectively. According to GB 18306-2015, the peak ground acceleration (PGA) of DBE for the site of the prototype building is 0.2 g. The site of the prototype building falls into Site Class III, with an average shear wave velocity in the top 30 m of soil, V_{S30} , between 150 m/s and 250 m/s. The characteristic period of seismic spectra, T_g , is 0.45 s.

3.1.2. Selection and scaling of ground motions. Ground motion records are selected such that

their spectral shape is similar to the target spectra considered in the assessment. The target spectrum for record selection is the DBE design response spectrum. In order to select ground motions to match the target spectrum, the NGA West 2 Ground Motion Database [25] is used for record selection. Record characteristics with magnitudes greater than 6, average shear wave velocity consistent with Site Class III and no restriction on fault type and fault distance are used to search the database. The records are linearly scaled to match the target spectrum, and they are selected such that the computed mean squared error (MSE) of their response spectra (assuming 5% damping) of the suite average is minimized with respect to the target spectrum over the period range of interest. As recommended by Qu et al. [26], the period range of interest is selected to span from 0.1 s to T_g , the characteristic site period, and from T_1 minus 0.2 s to $2T_1$, where T_1 is the fundamental period of the structure. The selected ground motion records, individual record spectra, the mean spectrum of the selected records and the target spectrum plotted against the period range of interest are shown in Figure 7. The suite contains seven ground motion records, which are sufficient when the fit between the ground motion spectra and the target spectra is good [27] and the goal of the assessment is to estimate mean values of response [28].



(a) Target spectra and response spectra of scale motions at DBE

(b) Acceleration time histories of scale motions at DBE

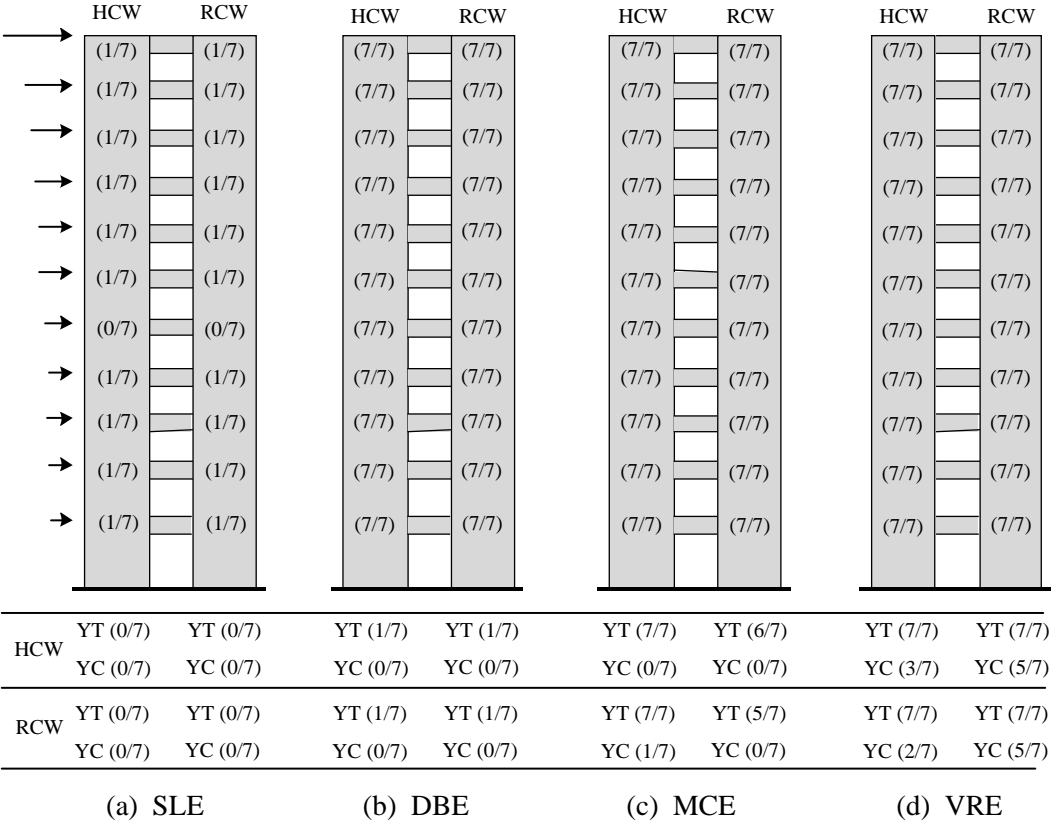
Figure 7. Selected ground motion records and response spectra.

3.1.3. Analysis assumption and dynamic parameters. The selected ground motions are input at the base of the coupled wall models, which are assumed to be fixed at their base. Following the recommendations in GB 50011-2010 [6], a damping ratio of 5% is assumed in the analysis, implemented using the Rayleigh damping model for the first and third vibration modes of the coupled walls.

3.2. Dynamic analysis results

3.2.1. Yield mechanism. Figure 8 compares yield mechanisms of the HCW and the RCW. The coupling beams are designed to satisfy strength demands under SLE. Therefore, very few RSCBs and RC coupling beams yield when subjected to the SLE records, while all RSCBs and RC coupling beams yield when subjected to the DBE, MCE and VRE records. The minimum requirement of Chinese code on boundary longitudinal reinforcement results in a flexural strength of these wall piers twice their SLE strength demand. As a result, for both the HCW and the RCW, no wall piers yield when subjected to all SLE motions as well as most of

DBE motions. Both wall piers yield under combined axial forces and bending moments when subjected to most of the MCE motions and all VRE motions.



Notice: The numbers on the coupled walls show the number of ground motions which cause the coupling beam to yield. The numbers beneath the coupled walls show the number of ground motions which cause the longitudinal bars in the wall piers to yield. YT means rebars yield in tension and YC means rebars yield in compression.

Figure 8. Yield mechanism of the HCW and the RCW.

3.2.2. *Strength demands.* Figure 9 provides a comparison between the shear forces of coupling beams distributed along the height of the HCW and the RCW. Both mean values and 84th percentile values (i.e., mean value plus one standard deviation) of the responses are provided in this figure. When subjected to SLE records, the mean values of beam shear forces are below the nominal shear strength of the coupling beams. When subjected to DBE records, all coupling beams yield, slight overstrength is observed in the RC coupling beams, while RSCBs develop considerable overstrength. When subjected to MCE and VRE, the RSCBs show significantly greater overstrength than the RC coupling beams.

Figure 10 shows the hysteretic responses of coupling beams at the 11th story when subjected to the Codroipo motion at VRE. Besides the large overstrength factor, the RSCB also shows full hysteretic loops and large energy dissipation, while the RC coupling beam shows hysteresis properties with evident pinching effects and stiffness degradation. Therefore the coupling action of the RCW is reduced under severe earthquakes, which would lead to the degradation of entire lateral stiffness and larger lateral drifts than the HCW.

Figure 11 shows the variation of base shear versus axial force in the right wall pier when subjected to the Codroipo motion at MCE and VRE. The shear strength of the wall is calculated following GB 50010-2010 [6]. For both the HCW and the RCW, the base shear is

far less than shear strength of the wall pier, and no shear failure occurs. Figure 12 shows the variation of moment versus axial force at the base of the right wall pier when subjected to the Codroipo motion at MCE and VRE. The wall pier of the HCW bears larger variation of axial force, while the wall pier of the RCW bears larger variation of bending moments. The larger variation of axial force in the wall pier of the HCW than that of the RCW is mainly due to the stable hysteretic responses and large overstrength of the RSCBs. In the HCW, the stable responses and overstrength of RSCBs post yielding of shear links increase the coupling action of the system which in turn increases the tensile and compressive forces acted on the wall piers, whereas in the RCW, stiffness degradation of the RC coupling beams decreases the coupling action and thus the wall piers have to carry increased bending moments.

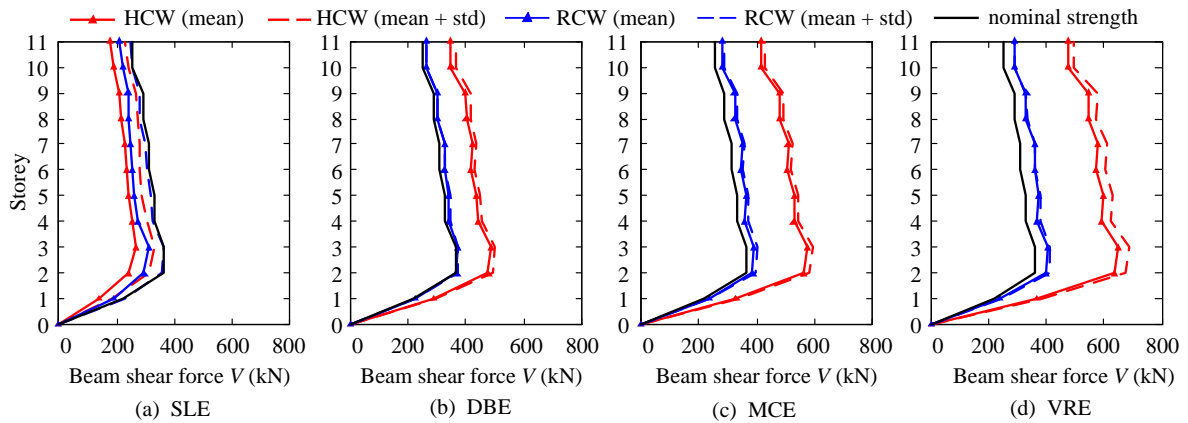


Figure 9. Beam shear force demands for the HCW and the RCW.

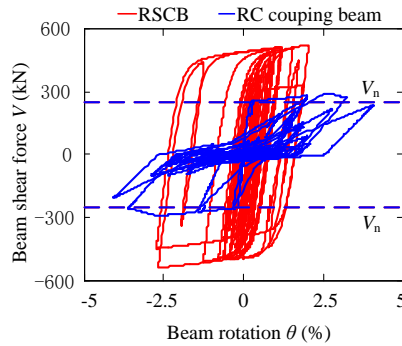


Figure 10. Hysteretic response of a sample RSCB and RC coupling beam at VRE.

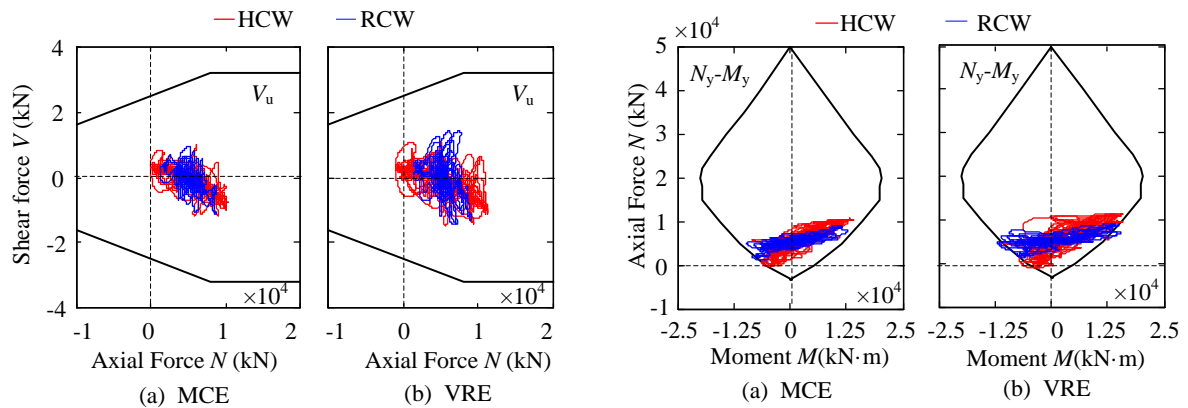


Figure 11. N - V relationship of wall piers in

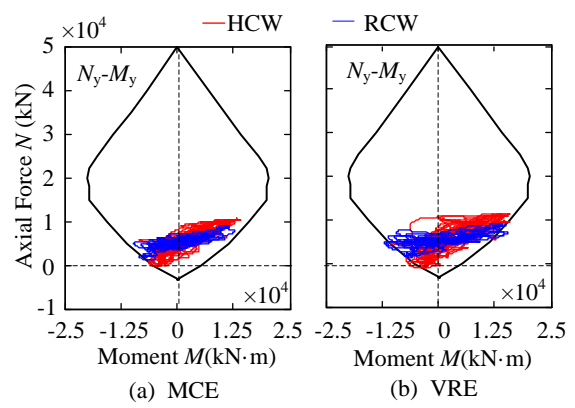


Figure 12. N - M relationship of wall piers in

the HCW and the RCW subjected to Codroipo motion at MCE and VRE.

the HCW and the RCW subjected to Codroipo motion at MCE and VRE.

3.2.3. *Deformation.* Figure 13 compares the peak transient interstory drift distribution of the HCW and the RCW. The maximum interstory drift ratio appears at the top stories for both systems. When subjected to SLE records, the interstory drifts are almost identical for both systems with maximum values around 1/800, i.e., the drift limit required by GB 50011-2010 [6]. When subjected to DBE, MCE and VRE, the maximum interstory drift ratios of the HCW are 16%, 29% and 31% smaller than those of RCW, respectively. This is attributed to the fact that under large deformation, the RSCBs show stable hysteretic response with large energy dissipation and overstrength, while the RC coupling beams present little overstrength and significant stiffness degradation.

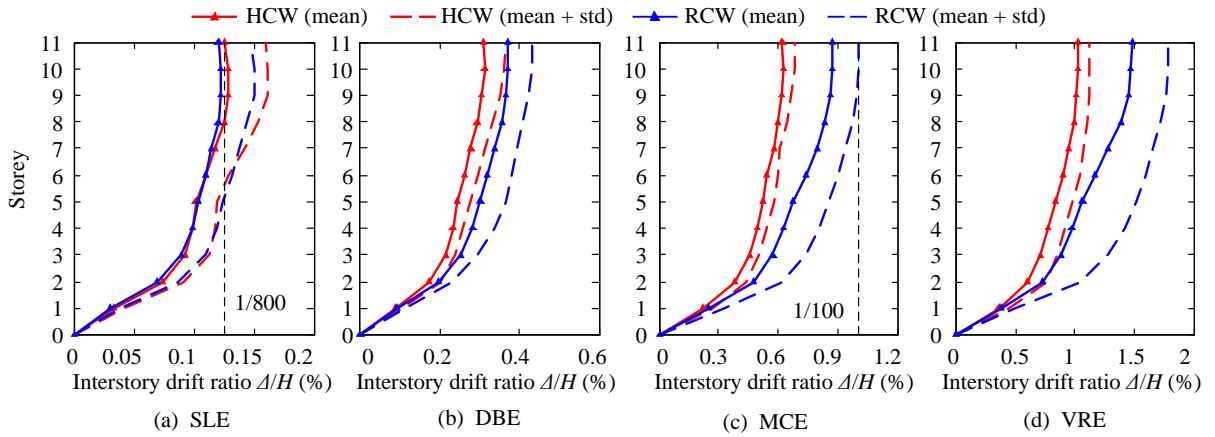


Figure 13. Mean interstory drift ratios of the HCW and the RCW.

Figure 14 compares the beam rotation distribution of the HCW and the RCW. When subjected to SLE records, the beam rotations are nearly identical for both the RSCBs and the RC coupling beams. When subjected to DBE, MCE and VRE records, the maximum beam rotations of the RSCBs are 24%, 36% and 42% smaller than those of the RC coupling beams respectively, due to larger energy dissipation and overstrength of the RSCBs. Even under VRE, the maximum chord rotations of the shear links in the RSCBs are 0.086 rad, which are less than the inelastic rotation capacity $\gamma_p = 0.14$ suggested by Ji et al [5] for shear links with a length ratio less than 1.0.

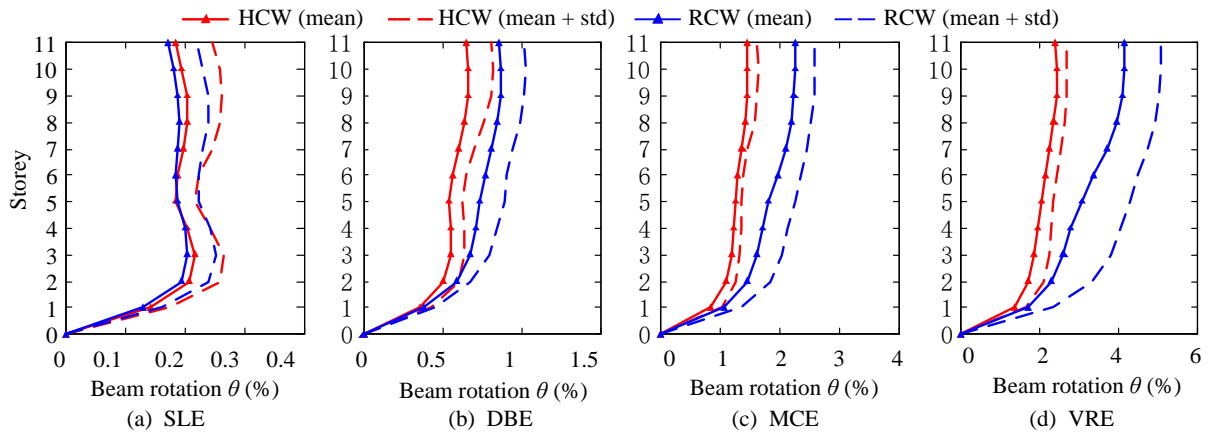


Figure 14. Mean beam rotations of the HCW and the RCW.

4. ASSESSMENT OF SEISMIC PERFORMANCE

This section assesses the expected seismic damage and suggests associated repair methods for both coupled wall systems based on the estimated responses under four intensities of ground motion shaking. The results can provide an indicator for enhanced performance and reparability of the new HCW system against earthquake hazards when compared with the traditional RCW system. The method for seismic damage assessment refers to a recently developed guideline of FEMA P-58 [27].

4.1 Structural components fragility data

Seismic performance assessment requires basic knowledge of the fragility data of building components. A component fragility function is a statistical distribution that indicates the conditional probability of incurring damage at a given value of demand parameter, which is typically assumed to be lognormal distribution. Component fragility functions contain unique fragilities for each possible damage state in the component. As described below, fragility functions for the RSCBs are proposed based on recent experiments conducted by Ji et al. [3,5]. For RC wall piers and RC coupling beams, the fragility curves recommended in FEMA P-58 are used as such data is not yet available in Chinese codes and standards. However, it is noted that the GB 50011-2010 provisions for conventional RC coupling beams are similar to those in ACI 318-14 [29], and therefore the RC coupling beams designed in accordance with both codes are expected to have similar fragility curves. The RC walls designed by GB 50011-2010 appear to have less boundary transverse reinforcement than the special walls designed by ACI 318-14. Preliminary analysis on a large volume of slender RC wall test data from China indicates that their fragility curves of DS1 and DS2 (minor to moderate damage) are nearly identical to FEMA P-58 curves, while the median wall drift corresponding to DS3 and DS4 (severe damage) is somewhat smaller than the values suggested in FEMA P-58.

4.1.1 RC walls. FEMA P-58 [27] provides fragility functions for slender RC shear walls (aspect ratio ≥ 2.0) (Fragilities B1044.091 to B1044.113). Due to its simplicity of calculation and good correlation to damage observed in the tests, in this study effective wall drifts (EWD) are selected as the demand parameter in the fragility functions to estimate different damage levels to the walls. Note that, interstory drift can also be used as the demand parameter for the fragility functions. However, directly using individual story drift data to estimate wall damage at every story is inaccurate, as often times in shear wall systems, the large drifts obtained at higher stories are a result of rigid body rotation of the top stories induced by damage to the wall near its base. Table V provides a summary of the median values and dispersions associated with the slender shear wall fragility, damage state descriptions and associated repair measures, as well as a visual illustration of the damage level for each damage state.

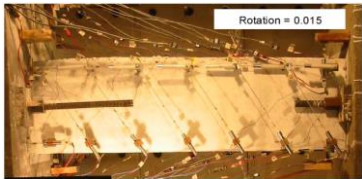
Table V. Summary of slender RC wall fragility data. Source: FEMA P-58 [27].

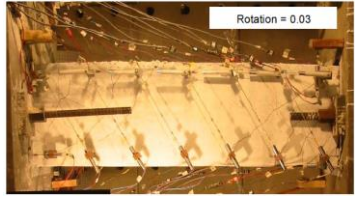
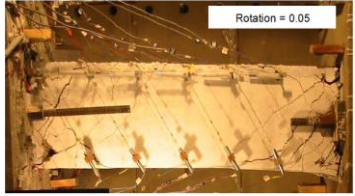
Damage state	Fragility data	Damage description	Repair method	Extent of damage
--------------	----------------	--------------------	---------------	------------------

DS1	Median: 0.0012 (EWD) Dispersion: 0.76	Formation of initial cracking. Crack width <0.02 in (0.5mm).	Cosmetic repair of surface finish to maintain first resistance and prevent water infiltration.	
DS2	Median: 0.0093 (EWD) Dispersion: 0.48	Spalling of concrete cover. Appearance of vertical cracks. Crack width >1/16 in (1.6 mm).	Epoxy injection of cracks and patching of spalled concrete.	
DS3	Median: 0.013 (EWD) Dispersion: 0.34	Exposure of longitudinal wall reinforcement.	Shoring of the wall and removing and replacing all concrete in the damaged region.	
DS4	Median: 0.019 (EWD) Dispersion: 0.44	Crushing of concrete. Buckling or fracture of reinforcement.	Replacement of the wall or concrete jacketing.	

4.1.2 RC coupling beams. FEMA P-58 [27] provides fragility functions for RC coupling beams for a variety of aspect ratios, thicknesses and reinforcement layouts (diagonally and conventionally reinforced). Beam rotation is the demand parameter utilized in the fragility functions. In the structure considered in this study, RC coupling beams are conventionally reinforced, with a thickness of 350-400 mm and an aspect ratio of 2.4. Consistent with those beam properties, FEMA P-58's fragility B1042.002b is selected to best represent these structural components. Table VI provides a summary of the median values and dispersions associated with the RC coupling beam fragility, damage state descriptions and associated repair measures, as well as a visual illustration of the damage level for each damage state.

Table VI. Summary of RC coupling beam fragility data. Source: Naish et al. [8].

Damage state	Fragility data	Damage description	Repair method	Extent of damage
DS1	Median: 0.014 (rad) Dispersion: 0.21	Appearance of residual cracks no greater than 1/16 in (1.6 mm). Limited flexural cracking.	Epoxy injection of cracks.	

S2	Median: 0.026 (rad) Dispersion: 0.33	Appearance of residual cracks greater than 1/8 in (3.2 mm) and minor spalling of concrete.	Epoxy injection of cracks and replacement of spalled concrete.	
DS3	Median: 0.041 (rad) Dispersion: 0.75	Significant strength degradation. Buckling and fracture of reinforcement. Crushing of concrete.	Removing and replacing damaged concrete and reinforcement.	

The fragilities here presented make no consideration of damage to the slabs above the RC coupling beams. While researchers have studied the impact of the slab on the load-deformation response of RC coupling beams [8], these findings have not been incorporated into the fragility functions available in the literature.

4.1.3 RSCBs. Similar as eccentrically braced frames (EBFs), link rotation is taken as the demand parameter utilized in the fragility functions of RSCBs. Three distinct damage states are observed in the specimens considered. Figure 15 illustrates the experimental and fitted fragilities proposed for the RSCBs. The method of maximum likelihood is used to develop the fragility curves for the RSCBs. This method finds the parameters such that the resulting distribution has the highest likelihood of having produced the observed data [27]. Table VII provides a summary of the median values and dispersions associated with the RSCB fragility, damage state descriptions and associated repair measures, as well as a visual illustration of the damage level for each damage state. It is notable that the yielding of link is regarded as DS0 (no damage), as the structural repair is not necessary and the shear strength and stiffness of the component are not affected. Note that test data associated with DS1 is limited to a handful of samples with different connection details of the RC slab to the RSCB. Median rotation demands at which the slab requires replacement are obtained from the limited dataset. The estimated mean is close to the values reported in FEMA P-58 [27] for slab replacement above shear links in EBFs.

Table VII. Summary of RSCB fragility data.

Damage state	Fragility data	Damage description	Repair method	Extent of damage
DS1	Median: 0.05 (rad) link rotation Dispersion: 0.3	Damage to the slab above the RSCB, with no damage to the RSCB itself.	Replacement of the portion of the slab above the RSCB.	

DS2	Median: 0.09 (rad) link rotation Dispersion: 0.19	Buckling of the web or flanges in the shear link.	Heat straightening buckled elements or replacement of shear link.	
DS3	Median: 0.11 (rad) link rotation Dispersion: 0.15	Fracture of the web in the shear link or fracture of the flange-to-end plate welds.	Replacement of the shear link.	

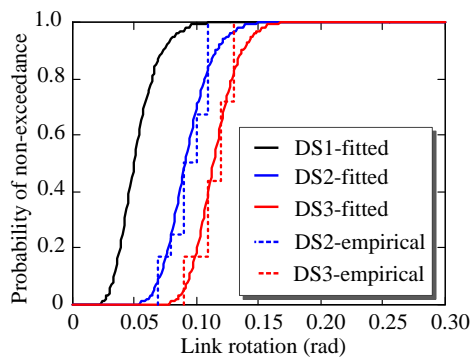


Figure 15. Fragility functions for RSCBs

4.2 Performance Assessment

The seismic performance of the HCW and the RCW are assessed based on the residual deformation acceptance criteria and the fragility functions for the structural components. The comparison is conducted based on mean estimates of response under at DBE, MCE and VRE. An evaluation at SLE is not considered as all structural components remain elastic at this intensity of shaking, i.e. there is no damage. Residual drifts are an important indicator of reparability given that in the presence of large residual drifts, a structure may be deemed irreparable due to the technical and economic feasibility of repair. In accordance with FEMA P-58 [27], the median residual drifts of 0.2% in buildings implies no structural realignment is necessary (although repairs may be required for nonstructural components). Table VIII summarizes the mean values of the maximum residual drifts of all stories in both the HCW and the RCW system. Both system comply with the recommendations of FEMA P-58 [27] to ensure no structural realignment is required.

Regarding the performance of structural components, damage to the RC wall piers is very limited in both the HCW and the RCW, even under VRE events. In this study, damage to the shear walls is concentrated in the lower two stories. Therefore, the effective wall drift was computed using an effective wall height equal to the first two stories. Table VIII summarizes the effective mean wall drifts in the HCW and the RCW. Figure 16 illustrates the probabilities of observing different damage levels in the wall piers under DBE, MCE and VRE where DS0

denotes no damage. At DBE and MCE expected damage in both systems is effectively identical, with large probabilities of observing DS1 (55-60% and 88-90% respectively) requiring surface finish repairs. Under VRE, expected damage between the two systems is still comparable, though greater probability of observing DS2 is observed for the RCW (14%) than the HCW (8%), which would require epoxy injecting of cracks and patching spalled concrete. Overall, expected damage is very low due to the high structural stiffness required by Chinese codes.

Table VIII. Mean residual story drifts and effective wall drifts for the HCW and the RCW.

Earthquake level	Residual story drifts (%)		Effective wall drifts (%)	
	HCW	RCW	HCW	RCW
DBE	0.013	0.007	0.13	0.15
MCE	0.025	0.013	0.30	0.37
VRE	0.070	0.039	0.48	0.56

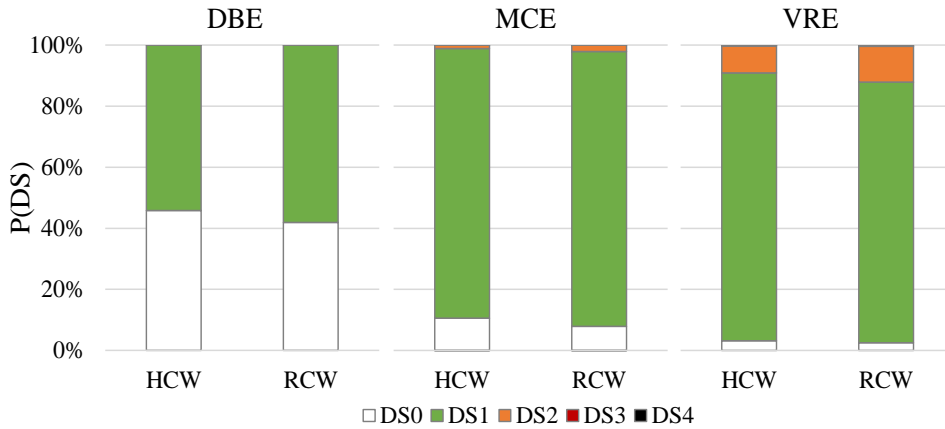


Figure 16. Expected damage in the wall piers of the HCW and the RCW.

Figure 17 illustrates the probability of observing different damage states for the RSCBs and the RC coupling beams along the building height, where DS0 denotes no damage. Under DBE, though yielded, the beams are effectively undamaged. Under MCE, the RSCBs show high probabilities of no damage (54-99% probability of DS0), whereas the RC coupling beams illustrate significant probabilities of limited damage, particularly in the upper stories (66-72% probability of DS1), and probabilities of moderate damage (DS2) and severe damage (DS3) in the order of 16-21% and 10-13% respectively in the top 5 stories. Under VRE, RSCBs have high probabilities of incurring DS1, with values of up to 78%, and probabilities of moderate damage (DS2) in the order to 21-36% in the top 5 stories. Ji et al. [3] report that with residual beam rotation less than 0.45%, damaged links can be readily replaced if the RSCBs adopt specialized link-to-beam connections. The mean value of the maximum residual beam rotation under VRE is 0.23%, and therefore the shear link can be easily replaced if necessary. On the other hand, the RC coupling beams, particularly in the upper stories, illustrate significant probability of moderate to severe damage (38-42% and 45-55% probabilities of DS2 and DS3 respectively). These results illustrate how the RSCBs have

enhanced performance over the RC coupling beams under the strong earthquake motions. Under MCE and VRE, the RSCB repairs are limited to replacement of the portion of the slabs above RSCBs and possible replacement of shear links, whereas RC coupling beam repairs would require removing and replacing damaged concrete and reinforcement.

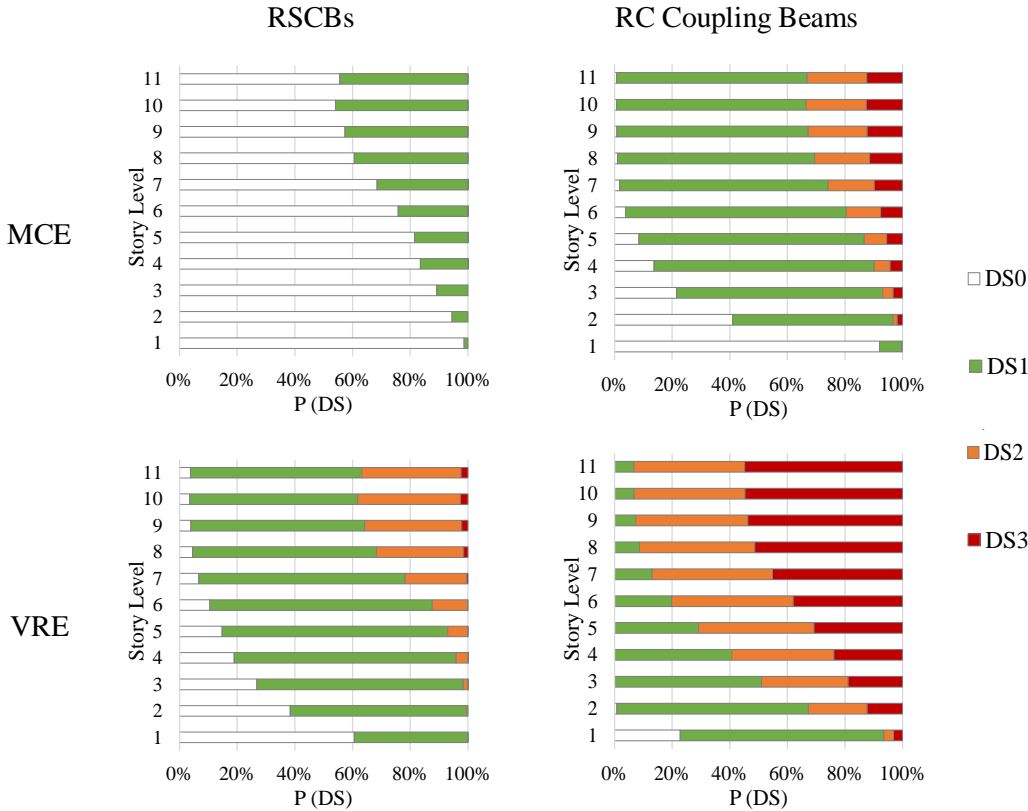


Figure 17. Expected damage in the RSCBs and the RC coupling beams.

5. CONCLUSIONS

This study assesses the seismic performance of a HCW system with RSCBs at four intensities of ground motion shaking as defined in the Chinese code: SLE, DBE, MCE and VRE. The performance of the HCW system is benchmarked against the traditional RCW with RC coupling beams. Nonlinear numerical models are developed in OpenSees for a representative wall elevation in a prototype 11-story building located in Beijing and designed per modern Chinese standards.

The results indicate that behavior of the two systems is consistent at SLE, where both systems remain elastic and DBE, where all coupling beams yielded, yet the walls remained elastic. At MCE and VRE, due to significant stiffness degradation of RC coupling beams, the coupling action of the RCW is reduced and a relatively larger portion of overturning moment is resisted by the wall piers, resulting in larger drifts in RCW than in the HCW. The maximum interstory drifts are 29% smaller at MCE and 31% smaller at VRE in the HCW than in the RCW. At MCE and VRE, the maximum beam rotations of the RSCBs are 36 to 42% smaller than those of the RC coupling beams.

Expected damage to the walls, even under extreme events, is limited to cracks and slight spalling of concrete, which only require surface repairs for both the HCW and the RCW. Whereas no damage is expected in the beams under SLE and DBE, some damage is expected

in both the RSCBs and the RC coupling beams under MCE and VRE. At these intensities, expected damage to the RSCBs is limited to the slab above the RSCB and possible web buckling of the shear link, whereas damage to the conventional RC coupling beam would result in cracks, spalling and crushing of concrete, buckling and fracture of reinforcement, particularly in coupling beams in the upper stories. Overall, under extreme earthquake events, the HCW with RSCBs illustrates enhanced performance over the conventional RCW with RC coupling beams, as it can quickly recover by easily replacing the damaged links as opposed to conducting costly and time consuming repairs of RC coupling beams.

ACKNOWLEDGMENTS

The work presented in this paper was sponsored by the International Science & Technology Cooperation Program of China (Grant No. 2014DFA70950), the National Natural Science Foundation of China (Grants No. 51261120377) and by Tsinghua University Initiative Scientific Research Program (Grant No. 2012THZ02-1). The authors wish to express their sincere gratitude to the sponsors.

REFERENCES

- [1] Fortney P J, Shahrooz B M, Rassati G A. Large-scale testing of a replaceable “fuse” steel coupling beam. *Journal of Structural Engineering* 2007, **133**(12): 1801-1807.
- [2] Christopoulos C, Montgomery M S. Viscoelastic coupling dampers (VCDs) for enhanced wind and seismic performance of high-rise buildings. *Earthquake Engineering & Structural Dynamics* 2013, **42**(15): 2217-2233.
- [3] Ji X, Wang Y, Ma Q, Taichiro O. Cyclic behavior of replaceable steel coupling beams. *Journal of Structural Engineering (ASCE)* 2015, under review.
- [4] Okazaki T, Arce G, Ryu H C, Engelhardt M D. Experimental study of local buckling, overstrength, and fracture of links in eccentrically braced frames. *Journal of Structural Engineering (ASCE)* 2005, **131**(10): 1526-1535.
- [5] Ji X, Wang Y, Ma Q, Okazaki T. Cyclic behavior of very short steel shear links. *Journal of Structural Engineering (ASCE)* 2016, **142**(2): 04015114.
- [6] CMC (Ministry of Construction). *Code for Seismic Design of Buildings (GB 50011-2010)*. Beijing: China Architecture & Building Press, 2010.
- [7] CMC (Ministry of Construction). *Technical Specification for Concrete Structures of Tall Building (JGJ 3-2010)*. Beijing: China Ministry of Construction, 2010 (in Chinese).
- [8] Naish D, Fry A, Klemencic R, et al. Reinforced concrete coupling beams-Part I: testing. *ACI Structural Journal* 2013, **110**(6): 1057.
- [9] Harries K A. Ductility and deformability of coupling beams in reinforced concrete coupled walls. *Earthquake Spectra* 2001; **17**(3): 457-478.
- [10] El-Tawil S, Kuenzli C M. Pushover of hybrid coupled walls. II: Analysis and behavior. *Journal of Structural Engineering (ASCE)* 2002; **128**(10): 1282-1289.
- [11] AISC. *Seismic Provisions for Structural Steel Buildings (ANSI/AISC 341-10)*. Chicago: American Institute of Steel Construction, 2010.
- [12] OpenSEES. *Open System for Earthquake Engineering Simulation*. Pacific Earthquake

- Engineering Research Center. (Available from <http://opensees.berkeley.edu/>) [accessed on January 15, 2015].
- [13] Lu X, Xie L, Guan H, Huang Y, Lu X. A shear wall element for nonlinear seismic analysis of super-tall buildings using OpenSees. *Finite Elements in Analysis and Design* 2015; 98: 14-25.
- [14] Ji X, Sun Y, Qian J, Lu X. Seismic behavior and modeling of steel reinforced concrete (SRC) walls. *Earthquake Engineering & Structural Dynamics* 2015, **44**(6):955-972.
- [15] Kent DC, Park R. Flexural members with confined concrete. *Journal of the Structural Division* 1971; **97**(7): 1969-1990.
- [16] Saatcioglu M, Razvi SR. Strength and ductility of confined concrete. *Journal of Structural Engineering (ASCE)* 1992; **118**(6): 1590-1607.
- [17] OpenSees Wiki. Steel02 Material -- Giuffr -Menegotto-PintoModel with Isotropic Strain Hardening.
[http://opensees.berkeley.edu/wiki/index.php/Steel02_Material_--_Giuffr -Menegotto-Pinto_Model_with_Isotropic_Strain_Hardening](http://opensees.berkeley.edu/wiki/index.php/Steel02_Material_--_Giuffr%C3%A9-Menegotto-Pinto_Model_with_Isotropic_Strain_Hardening) [Accessed on January 15, 2015].
- [18] Sun Y. *Study on Seismic Behavior of Hybrid Coupled Wall with Replaceable Steel Coupling Beams*. Master's thesis, Beijing: Tsinghua University, 2015 (in Chinese).
- [19] ASCE/SEI. *Seismic Evaluation and Retrofit of Existing Buildings (ASCE/SEI 41-06)*. Reston, VA: Structural Engineering Institute, 2014.
- [20] Kwan A K H, Zhao Z Z. Cyclic behaviour of deep reinforced concrete coupling beams. *Structures and Buildings* 2002; **152**(3): 283-293.
- [21] Gong Binnian, Fang Ehua. Behavior of reinforced concrete coupling beams between shear walls under cyclic loading. *Journal of Building Structures* 1988, **01**:34-41 (in Chinese).
- [22] Hassan M, El-Tawil S. Inelastic dynamic behavior of hybrid coupled walls. *Journal of Structural Engineering* 2004; **130**(2): 285-296.
- [23] Ji X, Wang Y, Zhang J, Okazaki T. Seismic behavior and fragility curves of replaceable steel coupling beams with RC slabs. *Journal of Structural Engineering (ASCE)* 2016, under review.
- [24] Standardization Administration of China (SAC). *Seismic ground motion parameters zonation map of China (GB 18306-2015)*. Beijing: Standards Press of China (in Chinese).
- [25] PEER NGA-West2 Database. Pacific Earthquake Engineering Research Center, Report No. 2013/03. Berkeley, CA: University of California, Berkeley, 2013
- [26] Qu Z, Ye L, Pan P. Comparative study on methods of selecting earthquake ground motions for nonlinear time history analyses of building structures. *China Civil Engineering Journal* 2011, **44**(7): 10-21 (in Chinese).
- [27] ATC. *Seismic Performance Assessment of Buildings Volume 1 – Methodology (FEMA P-58-1)*. Redwood City, CA: Applied Technology Council, 2012.
- [28] NIST. *Selecting and Scaling Earthquake Ground Motions for Performing Response History Analyses (NIST GCR 11-917-15)*. Washington, D.C.: National Institute of Standards and Technology, US Department of Commerce, 2011.

[29] ACI (American Concrete Institute). *Code Requirements for Structural Concrete (ACI 318-14) and Commentary*. American Concrete Institute: Farmington Hills, MI, 2014.